PNAS
www.pnas.org

# Supplementary Information for

## Snapping mechanics of the Venus flytrap (*Dionaea muscipula*)

**Renate Sachse**[1*†], **Anna Westermeier**[2,3**†], Max Mylo[2,3], Joey Nadasdi[4], Manfred Bischoff[1], Thomas Speck[2,3,5] and Simon Poppinga[2,5]

**Correspondence to:**
*sachse@ibb.uni-stuttgart.de (simulations)
**anna.westermeier@biologie.uni-freiburg.de (biological experiments)
†Contributed equally

**This PDF file includes:**

Supplementary text

Figures S1 to S4

Legends for Movies S1 to S24

**Other supplementary materials for this manuscript include the following:**

Movies S1 to S24



www.pnas.org/cgi/doi/10.1073/pnas.2002707117

**Supplementary Information Text: Equilibrium paths and snap-through**

Fig. S1 shows an equilibrium path for a three-hinged truss system (A1) that is loaded by the point load F and performs a snap-through process. The path (B) is derived from a quasi-static nonlinear analysis. Point L (A2) on the curve represents a limit point. It is characterized by a horizontal tangent and, therefore, zero stiffness of the displayed degree of freedom in the direction of the load.

After reaching (A2), there follows a *displacement-controlled* process with continuously increased displacement (A3-A6). During a *load-controlled* process, dynamic snap-through occurs, in which this part of the static equilibrium path is passed by, directly reaching a point beyond (A6).

Upon unloading, the process follows the static path in the reverse direction (C - green path - negative towards the y-axis) and reaches point A5, representing an alternative stress-free geometric configuration compared with the original geometry (A1). When a negative load is applied (C - orange path), a backward snap-through occurs. Subsequent unloading then reaches the starting point. Similar to loading, a snap-through can be avoided using a displacement control. Similar behavior can be observed in curved surfaces.

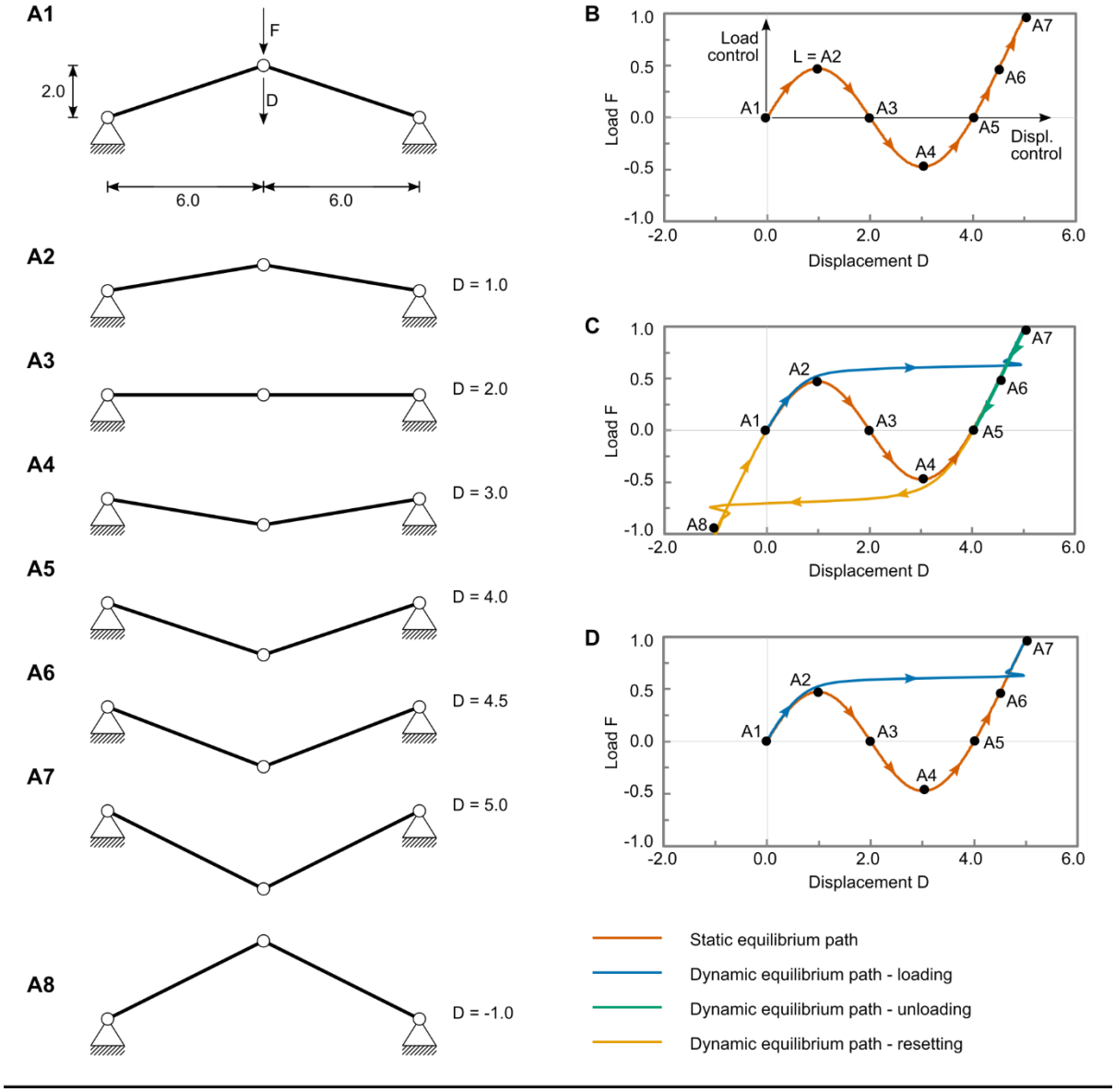


**Fig. S1:** Snap-through of a three-hinged structure. A1-A7) Deformation configurations in different load stages. A8) Deformation configuration after load inversion. B) Static equilibrium path. C) Dynamic equilibrium path for loading, unloading, and loading in the opposite direction (load inversion). D) Equilibrium path for dynamic loading and a displacement-controlled load inversion.

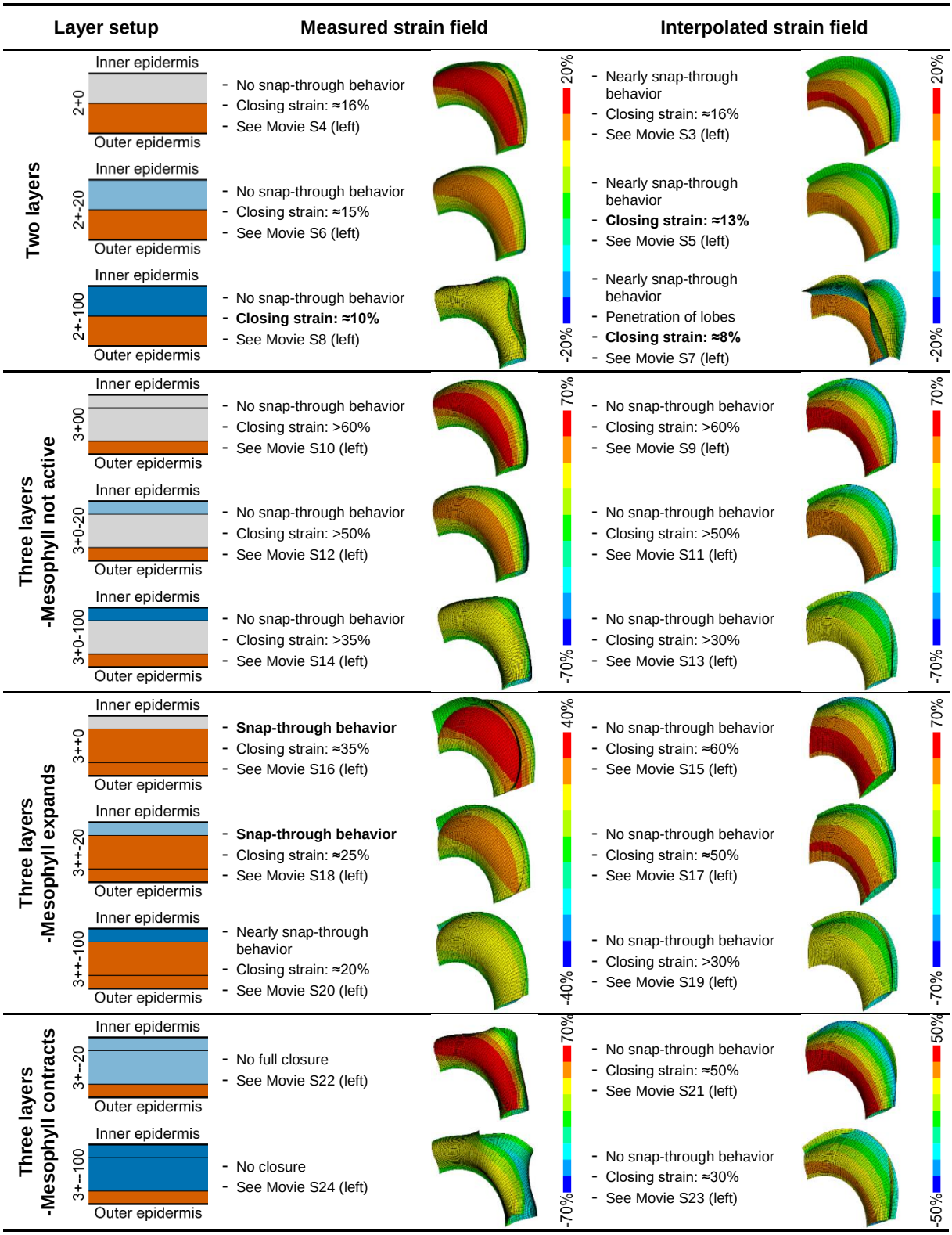


**Fig. S2:** Overview of simulation results for various layer setups/contributions and strain distributions (strain in x-direction – perpendicular to the midrib) not including the process of prestressing (model 1). Bold text indicates that this point in the simulation fits observations in experiments or realistic values. Model figures from Movies S3-24 left side.

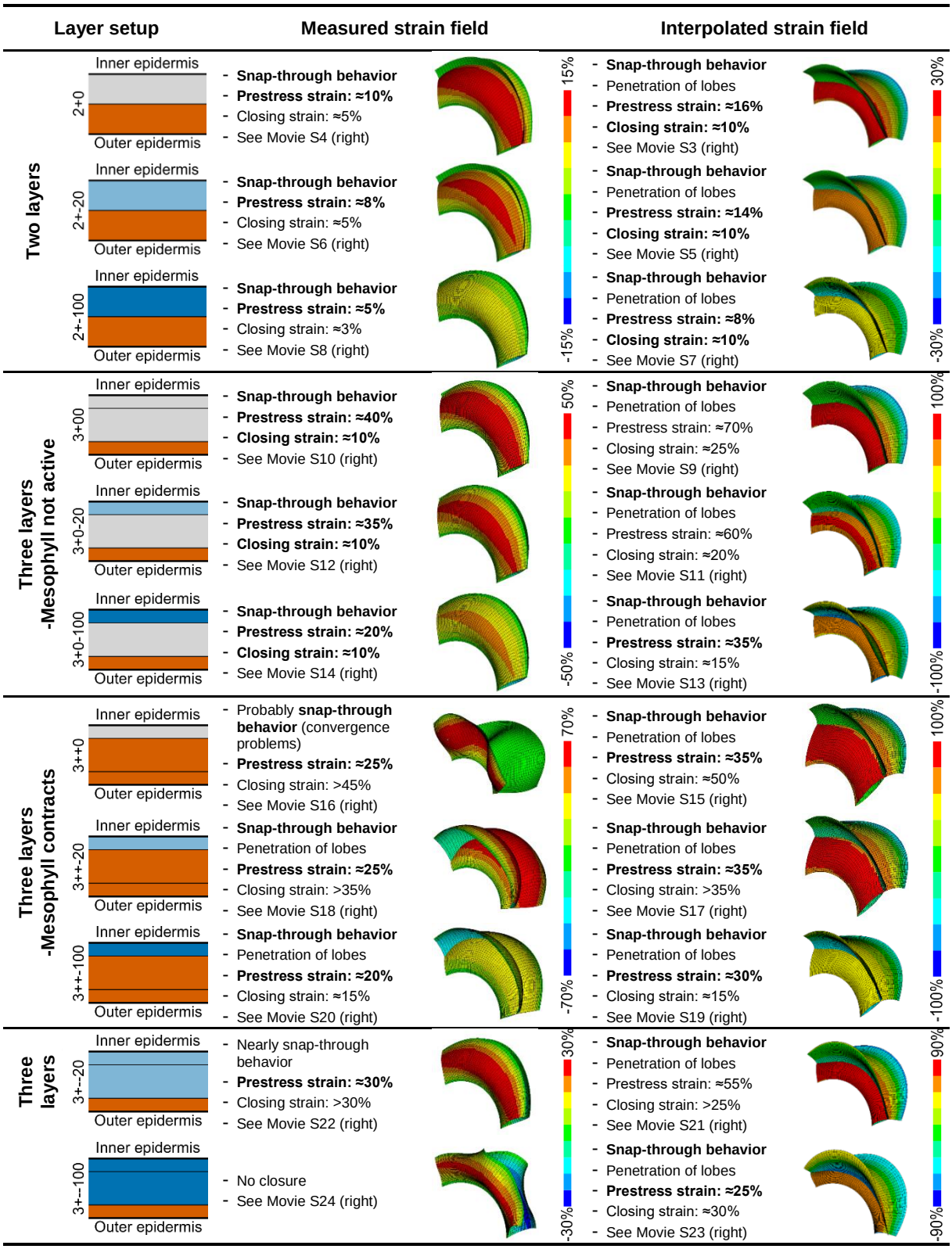


**Fig. S3:** Overview of simulation results for various layer setups/contributions and strain distributions (strain in x-direction – perpendicular to the midrib) including the process of prestressing (model 2). Bold text indicates that this point in the simulation fits observations in experiments or realistic values. Model figures from Movies S3-24 right side.

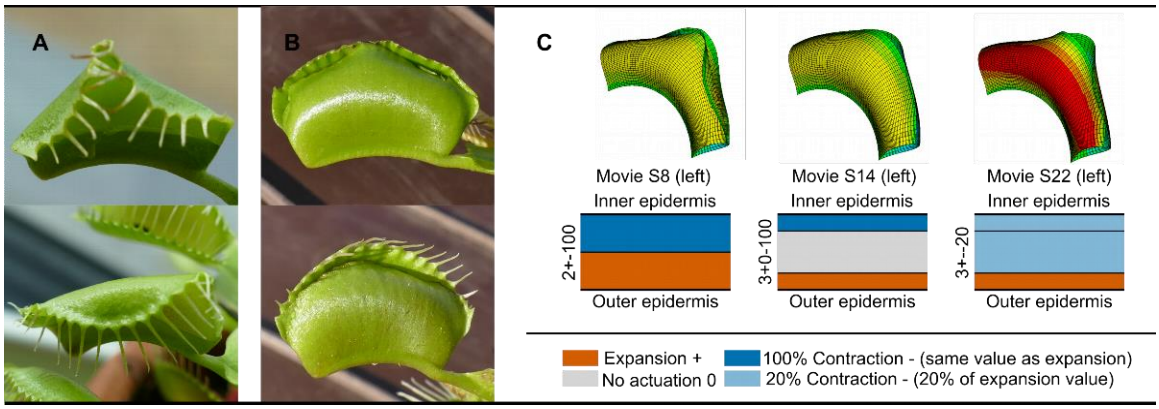


**Fig. S4:** Exaggerated lobe-bending behavior of real traps immediately after fast trap closure (i.e., after release of prestress) in which one lobe is cut off (A), the teeth (cilia) at the margins are removed (B), and computer models not including the process of prestressing in which no snap-through occurs (C).

**Movie S1 (separate file):** Strain distribution of the outer trap surface throughout fast snap-trapping, measured with DIC. Major strain – x-direction (left) and minor strain – y-direction (right).

**Movie S2 (separate file):** Strain distribution of the inner trap surface throughout fast snap-trapping, measured with DIC. Major strain – x-direction (left) and minor strain – y-direction (right).

**Movie S3 (separate file):** FE model with interpolated strain field for layer setup and –contribution 2+-0. Left: no prestress, right: with prestress.
**Movie S4 (separate file):** FE model with measured strain field for layer setup and –contribution 2+-0. Left: no prestress, right: with prestress.

**Movie S5 (separate file):** FE model with interpolated strain field for layer setup and –contribution 2+-20. Left: no prestress, right: with prestress.
**Movie S6 (separate file):** FE model with measured strain field for layer setup and –contribution 2+-20. Left: no prestress, right: with prestress.

**Movie S7 (separate file):** FE model with interpolated strain field for layer setup and –contribution 2+-100. Left: no prestress, right: with prestress.
**Movie S8 (separate file):** FE model with measured strain field for layer setup and –contribution 2+-100. Left: no prestress, right: with prestress.

**Movie S9 (separate file):** FE model with interpolated strain field for layer setup and –contribution 3+00. Left: no prestress, right: with prestress.
**Movie S10 (separate file):** FE model with measured strain field for layer setup and –contribution 3+00. Left: no prestress, right: with prestress.

**Movie S11 (separate file):** FE model with interpolated strain field for layer setup and –contribution 3+0-20. Left: no prestress, right: with prestress.
**Movie S12 (separate file):** FE model with measured strain field for layer setup and –contribution 3+0-20. Left: no prestress, right: with prestress.

**Movie S13 (separate file):** FE model with interpolated strain field for layer setup and –contribution 3+0-100. Left: no prestress, right: with prestress.
**Movie S14(separate file):** FE model with measured strain field for layer setup and –contribution 3+0-100. Left: no prestress, right: with prestress.

**Movie S15 (separate file):** FE model with interpolated strain field for layer setup and –contribution 3++0. Left: no prestress, right: with prestress.
**Movie S16 (separate file):** FE model with measured strain field for layer setup and –contribution 3++0. Left: no prestress, right: with prestress.

**Movie S17 (separate file):** FE model with interpolated strain field for layer setup and –contribution 3++-20. Left: no prestress, right: with prestress.
**Movie S18 (separate file):** FE model with measured strain field for layer setup and –contribution 3++-20. Left: no prestress, right: with prestress.

**Movie S19 (separate file):** FE model with interpolated strain field for layer setup and –contribution 3++-100. Left: no prestress, right: with prestress.

**Movie S20 (separate file):** FE model with measured strain field for layer setup and –contribution 3++-100. Left: no prestress, right: with prestress.

**Movie S21 (separate file):** FE model with interpolated strain field for layer setup and –contribution 3+--20. Left: no prestress, right: with prestress.
**Movie S22 (separate file):** FE model with measured strain field for layer setup and –contribution 3+--20. Left: no prestress, right: with prestress.

**Movie S23 (separate file):** FE model with interpolated strain field for layer setup and –contribution 3+--100. Left: no prestress, right: with prestress.
**Movie S24 (separate file):** FE model with measured strain field for layer setup and –contribution 3+--100. Left: no prestress, right: with prestress.